Initial steps in reactions of aquathermolysis of cyclohexyl phenyl sulfide by means of *ab initio* calculations

Y.V. Lysogorskiy *, R.M. Aminova, D.A. Tayurskii

Institute of Physics, Kazan Federal University, Kremlevskaya 18, Kazan 420008, Russia

ABSTRACT

Aquathermolysis is often proposed as a method to reduce the viscosity of heavy oils. In the present work we have investigated the aquathermolysis reaction of cyclohexyl phenyl sulfide in water medium by means of density functional theory. The water molecule was considered as a reagent and as a catalyst. We have shown that *ab initio* quantum chemistry methods could be applicable for comparative analysis of chemical reaction pathways in aquathermolysis processes. The obtained results could be useful for the systems like tert-alkyl (secondary-alkyl) thiophenyl ethers, which could be formed in heavy oils at harsh conditions. The scheme of different reaction directions with corresponding calculated values of reaction barriers, which are correlated with experimental data, is presented and could be used for comparison with other reaction mechanisms.

© 2016 Elsevier B.V. All rights reserved.

1. Introduction

The heavy oil production keeps increasing globally due to shortfall of conventional light crude oil. The heavy oil consists of high molecular mass compounds, including asphaltenes and resins, which are the main cause of high viscosity. Extremely high viscosity and an abundant amount of heteroatoms (S, O and N) in the structure of heavy oil molecules present major challenges for exploration, transportation and processing of heavy oil. Thus, in order to facilitate production, it is necessary to improve the rheological properties of heavy oil. This can be achieved either by increasing the temperature or by using special chemical transformations during heavy oil processing. One of the proposed methods to reduce the viscosity is aquathermolysis [1–3]. Aquathermolysis is a thermal cracking of large hydrocarbon molecules in the presence of water and in the absence of oxygen. The typical temperatures for aquathermolysis range from about 200 °C up to water critical point conditions (374 °C at 218 atm) [4]. The ability of water to carry out condensation, cleavage, and hydrolysis reactions can be explained by favorable changes in its chemical and physical properties, which at higher temperatures become more compatible with reactions of organic compounds. For example, the dissociation constant (K_W) of water as it approaches the critical point, is

about $10^{-11.30}$, which is about 3 orders of magnitude higher than the value at normal conditions ($10^{-13.99}$) [5], which makes the solvent properties of water at 250–350 °C comparable to properties of polar organic solvents at room temperature. Under those conditions water can act as either acidic or basic catalyst, and its reactivity can often be reinforced by autocatalysis from water-soluble reaction products [6]. Note, however, that once the critical point is passed the value of K_W decreases again dramatically [6].

Over the past decade, significant aquathermolysis processes researches have been focused on the development of the detailed reaction schemes and associated kinetic parameters (see [4] and references therein). However, most of the literature provides only qualitative insights into the chemical interactions of bitumen with steam condensate (or pure steam) while detailed studies of aquathermolysis reactions mechanisms at the molecular level are still relatively rare [7–9]. In Ref. [7] new mechanism for the catalyzed thermal decomposition of formic acid was proposed and analyzed by using B3LYP approach. It was established that decomposition barrier of HCOOH is lowered by 30% in the presence of one water molecule, by 50% in the presence of two water molecules and by 60% in the presence of another HCOOH molecule. In Ref. [8] the *ab initio* calculations of the standard enthalpies of formation, enthalpy of dissociation of the SH and gas-phase acidity for a large number of small sulfur-containing molecules in the gas phase at a temperature of 298.15 K were performed. In Ref. [9] the thermodynamic parameters of conversion reactions of some

* Corresponding author.
 E-mail addresses: yura.lysogorskii@gmail.com (Y.V. Lysogorskiy), rmaminova@gmail.com (R.M. Aminova), dtayursk@gmail.com (D.A. Tayurskii).

heavy oil components under the action of steam and heat were calculated using semiempirical PM6 method.

Our paper presents another systematic and in-depth study of aquathermolysis related chemical reaction mechanisms by using nonempirical quantum chemical methods. Out of a number of high molecular weight compounds that heavy oil consists of (asphaltenes, resins and other heavy hydrocarbons) we singled out cycloalkyl aryl sulfides as an object of our study for the following reasons. In general, cycloalkyl aryl sulfides have been identified as being responsible for forming abundant cross-link bridges within macromolecular network of heavy oil hydrocarbons [10] thus also being at least partially responsible for high heavy oil viscosity. The key feature of cycloalkyl aryl sulfides is know to be C–S heterobond. The cleavage of heterobonds in the presence of water could thus be one an important heavy oil viscosity reduction mechanism in the process of aquathermolysis [1,3].

Detailed experimental studies of chemical reactions of some compounds – cyclohexyl phenyl sulfide, in particular – with water, acids and liquid hydrocarbons were performed in Refs. [10–12], and a large number of reaction paths leading to a variety of products were identified.

To the best of authors' knowledge, the work presented here is the first quantum chemical investigation of the aquathermolysis of cyclohexyl phenyl sulfide. Here we have studied the mechanisms of initial steps of some cyclohexyl phenyl sulfide reactions: cleavage, hydrolysis and proton-catalyzed cleavage. Comparisons made between calculation results and available experimental data provide useful initial reference for applicability of different calculation methods in further studies.

2. Theoretical methods

The results presented in this paper were obtained by using GAUSSIAN 03 [13] and VASP [14–17] quantum chemistry computer codes.

Calculations using the GAUSSIAN 03 [13] program were based on density functional theory where PBE [18] and B3LYP [19,20] functionals were used with TZVP [21–23] basis set. In addition to these widely popular functionals, we also have used proposed in [24] ωB97X-D functional, which includes empirical atom–atom dispersion corrections. The ωB97X-D is known to yield satisfactory accuracy for thermochemistry, kinetics, and non-covalent interactions. In the GAUSSIAN program, we have found and calculated the energy and the structure of minima and transition states on the potential energy surface (PES) by performing an optimization of all geometrical parameters. Reliability of obtained transition states was confirmed by the identifying a single imaginary mode and by the calculations of the intrinsic reaction coordinate (IRC) [25].

In order to take into account the temperature effects, the Gibbs free energy was considered,

$$G = E_0 + E_{vib} + PV - T(S_{trans} + S_{rot} + S_{vib}), \qquad (1)$$

where E_0 is the electronic energy obtained from DFT calculations, E_{vib} is a zero point and vibrational energy, and S_{trans}, S_{rot} and S_{vib} are translational, rotational, and vibrational entropy contributions respectively. All thermodynamic quantities in Eq. (1) were calculated according to standard formulas given in textbook [26].

In general, aquathermolys processes, including the catalytic processes, take place in condensed phase and/or at the interface between solid and liquid phases. On the other hand, there are computer codes for studying the structures and properties of condensed matter, such as crystals, surfaces and other periodic systems. In the present paper, calculations based on density functional theory (DFT) methods within periodic boundary conditions were performed using Vienna Ab-initio simulation package (VASP

5.3) [14–17] integrated into MedeA software package.[1] The electron–ion interactions were described by using the projector-augmented wave (PAW) method. The PAW method is a frozen-core all-electron method that uses the exact shape of the valence electrons wave functions instead of pseudo-wave functions [27]. The H(1s), C($2s^2 2p^2$), O($2s^2 2p^4$) and S($3s^2 3p^4$) electrons of valence shell were treated explicitly, whereas remaining electrons of cores were taken into account by using pseudopotentials. Exchange and correlation effects were considered within the generalized gradient approximation (GGA). Several different functionals have been used in VASP calculations: PBE [18], PBE with semi-empirical dispersion-correction DFT-D approach proposed by Grimme [28] in order to account for dispersive Van der Waals interactions (below referred to as PBE + D2), and BLYP functional [19,29]. Plane waves (PW) were included up to a cutoff of 400 eV (further increasing of cutoff energy up to 600 eV did not result in significant changes of energy), and the Brillouin zone was sampled at its Γ-point. Convergence accuracy value of 10^{-6} eV was used to calculate electronic energies, and geometry relaxation was performed using the conjugate gradient method until the forces on atoms were less than 0.01 eV/Å. In the case of a charged system, an additional neutralizing background charge is applied by VASP and dipole and quadrupole corrections are taken into account. The simulation cell size was set to $15 \times 15 \times 15$ Å^3, and it was verified that further cell size increase leads to the energy changes of less than 0.25 kcal/mol. The vibrational properties within VASP were calculated using the MedeA-PHONON module, which implements a quasiharmonic approximation where the forces are calculated from the Hellmann–Feynman theorem [30] and six small frequencies associated with rotational and translational motion are eliminated.

The transition states (TS) of the reactions were determined using the nudged elastic band method [31], which is based on an explicit mapping of the reaction path. For each reaction a set of several images was used. It should be noted that this method is reliable only if there are no additional intermediate states between reagent and products of chemical reaction. In addition, the image closest to the transition state has been relaxed using a quasi-Newton algorithm to obtain the transition state. The transition states (TS) of the reactions were located by using the climbing image nudged elastic band method (CI-NEB) and additionally verified by using frequency analysis to identify a single imaginary mode associated with found TS.

Taking into account that the VASP program is widely used for studying the structures and properties of condensed matter, such as interaction of catalysts with surfaces, it was very interesting to compare the results obtained by VASP and GAUSSIAN programs for such quantities as free energy changes and reaction barriers. On the one hand, we have used a wide range of functionals for the exhaustive studying of chemical reactions, as is usual in quantum chemical researches. On the other hand, PBE functional is realized in both computer codes and it was used for direct comparison. In presented below comparison results we will denote the calculations done in GAUSSIAN by TZVP (reflecting the choice of TZVP basis for GAUSSIAN calculations). The calculations done in VASP will be denoted by 400 (referring to 400 eV plane wave basis cutoff energy).

3. Results and discussion

In order to study the reactions of cyclohexyl phenyl sulfide in water medium we have considered several reaction mechanisms as initial steps – homolytic cleavage, proton-catalyzed cleavage

---

and hydrolysis. The first two reactions were considered by Katritzky and co-authors as a possible reaction route of cyclohexyl phenyl sulfide aquathermolysis process [12], whereas the last one is studied for the first time in the present paper.

3.1. Verification of methods

In order to show the reliability of methods used, we have validated them by comparing the calculated dissociation energy of molecules containing S–S, S–C and S–H bonds with known experimental data [32]. The calculated values as well as experimental data and their comparison are given in Table 1. As one can see, the PBE level of theory gives the lowest average absolute error of energy obtained by using GAUSSIAN (2.83%) as well as by VASP programs (4.97%). So this functional will be used as a major one for further calculations of reactions including the C–S bond cleavage. At the same time, the comparison with other methods in some special cases also will be given.

3.2. Homolytic cleavage

The reactions of homolytic cleavage of C–S bond in cyclohexyl phenyl sulfide are shown on the reaction schemes as the R1 and R2. Both reactions are barrier-free. The Gibbs free energy changes for these reactions in a dependence on the temperature are shown in Fig. 1.

$$\text{(R1)}$$

$$\text{(R2)}$$
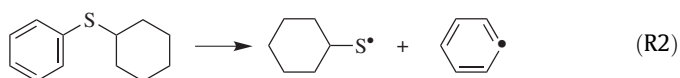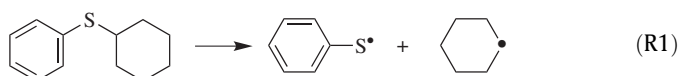
Reaction R1 has less value of Gibbs free energy change (about 50 kcal/mol) in comparison to reaction R2 (about 70 kcal/mol, see Fig. 1). The products of the reaction R1 could attach hydrogen and form thiophenol, which was experimentally detected in a significant amount (about 11 at.%), whereas only traces of cyclohexanethiol (about 0.3 at.%) were obtained [11,12,33]. Gibbs free energy changes for the reactions R1 and R2 are higher in comparison with ones considered below (proton catalyzed cleavage R3 and hydrolysis R4, R5), and such reaction paths should not be the major route in aquathermolysis processes at low temperatures. As was shown in Ref. [11], at 250 °C cyclohexyl phenyl sulfide underwent cleavage faster under aqueous conditions (ionic pathway) than under thermal conditions (radical pathway). However, with increasing the temperature such thermal cracking could become a dominant process.

### 3.3. Reaction of proton catalyzed cleavage

$$\text{(R3)}$$
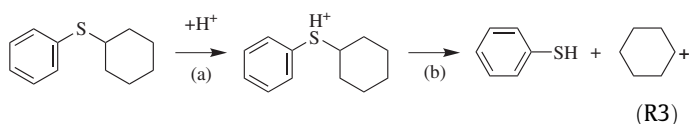
As was already mentioned, the dissociation constant of water as it approaches the critical point conditions is up to three orders of magnitudes higher, than for the normal conditions. Thus, the amount of hydrogen ions H^+ increases significantly and water can act also as an acid-catalyst. The hydrogen ion H^+ weakens the C–S bond and allows to break it with less energy costs. The hydrogen ion H^+ in water medium usually form the aqueous cation H_3O^+.

We have considered the interaction of one hydronium ion H_3O^+ with cyclohexyl phenyl sulfide (R3.a) and the subsequent cleavage of S–cyclohexyl bond (R3.b). It can be seen that as the result of full geometry optimization of reaction cluster consisted of hydronium ion and cyclohexyl phenyl sulfide the H^+ cation moves from hydronium ion towards S ion, see Fig. 2. Thus, the energy of the cluster is decreased with proceeding of the reaction R3.a. We are mostly interested in the reaction of cleavage of cyclohexyl phenyl sulfide R3.b, which is barrier-free reaction. The Gibbs free energy change (ΔG) of R3.b reaction is about 30 kcal/mol and decreases with increasing of temperature (see Fig. 3). The presence of hydrogen ion H^+ indeed decreases the activation energy of cleavage reaction which was proposed in previous experimental works by Katritzky et al. [33]. Acid-catalyzed (or proton catalyzed) reaction mechanism seems to be a major route in process of cyclohexyl phenyl sulfide aquathermolysis at the condition of sufficient hydrogen ion H^+ concentration.

3.4. Hydrolysis

Besides the reactions considered in previous works [11,33,12] we have studied the hydrolysis of cyclohexyl phenyl sulfide along two reaction paths (R4 and R5).

$$\text{(R4)}$$

$$\text{(R5)}$$
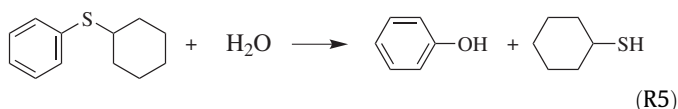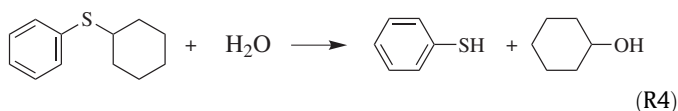
The transition states for both reactions (Fig. 4) were found. Validity of transition states founded was confirmed by the presence of a single imaginary frequency and the calculations of Internal Reaction Coordinate (IRC) [25]. The results of IRC calculations showed that downhill from the potential barrier top to one direction results to the geometrical structure of complex of cyclohexyl phenyl sulfide with one water molecule (see Fig. 5), and in another direction – to the structure of complex consisted of products for reactions R4 and R5 (see Fig. 6).

The energy diagram for these reactions $T = 298$ K and for $T = 523$ K is shown in Fig. 7. As one can see the high transition state energy (about 70 kcal/mol) indicates that such reactions are difficult to proceed. One can suppose, that presence of additional water molecules could significantly decrease the reaction barrier, as it already was shown in Ref. [7].

The dependencies on the temperature of Gibbs free energy changes ΔG as well as reaction barriers $\Delta G^{\neq}$ for reactions R4 and R5 with respect to the pre-reaction complexes (Fig. 5) for different functionals computed by using both codes (VASP and GAUSSIAN) are shown in Fig. 8. As one can see, the difference between free energy changes for given reactions calculated by different programs and several functionals is about 2 kcal/mol which is small enough and comparable to the experimental error. The values of the reaction barriers $\Delta G^{\neq}$ calculated by different approaches (Fig. 8b) show slightly larger scatter (about 10 kcal/mol), but demonstrate the similar tendencies for the reactions R4 and R5. Thus, comparative analysis shows that the results obtained by VASP are comparable with the results obtained by quantum chemical calculations on the good level of theory within GAUSSIAN program.

Table 1
Comparison of the S–S, S–C and S–H bond dissociation energy (kcal/mol) calculated by using of different DFT methods with experimental data.

	GAUSSIAN			VASP			
	PBE	B3LYP	ωb97XD	PBE	PBE + D2	BLYP	Exp. [32]
CH3SSCH3 → CH3SS + CH3	59.24	54.72	61.08	57.89	59.01	51.05	57.4 ± 1.5
CH3SSCH3 → 2∗CH3S	63.39	55.51	60.23	66.92	68.52	58.72	65.2 ± 0.9
HSSH → 2HS	65.58	57.38	61.15	65.66	66.18	57.44	64.7 ± 1.0
HSSH → HSS + H	72.76	74.80	76.37	64.11	64.43	64.55	76 ± 3.5
CH3SCH3 → CH3S + CH3	75.95	69.55	75.18	76.28	77.45	68.83	73.6 ± 0.8
CH3SH → CH3S + H	87.82	88.08	89.14	88.66	89.01	87.92	87.4 ± 0.5
CH3SH → CH3 + SH	78.88	72.10	77.11	81.25	81.73	73.48	74.7 ± 1.0
HSH → HS + H	92.69	92.22	93.15	95.96	96.13	94.35	91.10 ± 0.01
Ave. abs. error (%)	2.83	5.43	3.70	4.97	5.93	7.44	
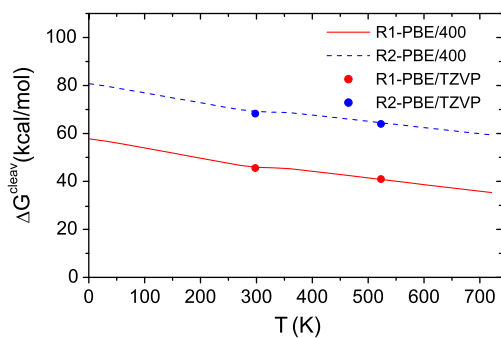
Fig. 1. The Gibbs free energy change (ΔG) for homolytic cleavage reactions (R1) and (R2) in a dependence on the temperature T (K).
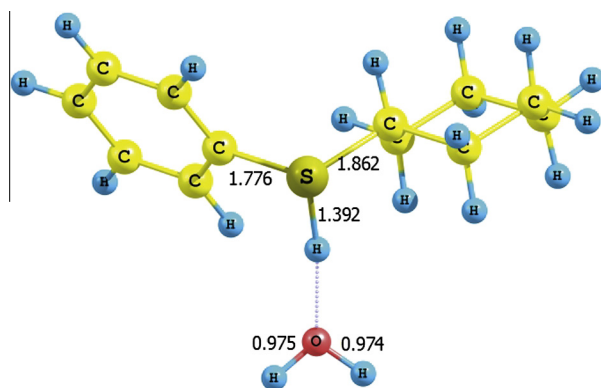
Fig. 2. The geometric structure of cyclohexyl phenyl sulfide with hydronium ion cluster after optimization at PBE/400 level of theory by using VASP program.
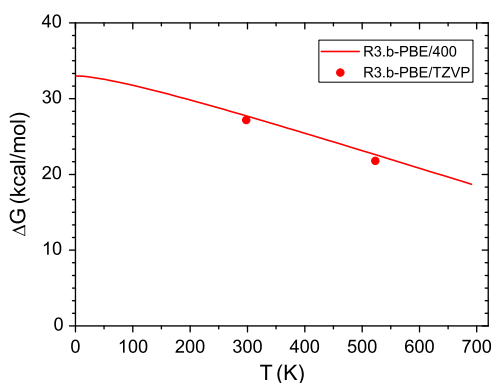
Fig. 3. The Gibbs free energy change ($\Delta G^{\neq}$) in proton-catalyzed cleavage reaction R3.b, calculated at the level of PBE/400 and PBE/TZVP in a dependence on the temperature T (K).
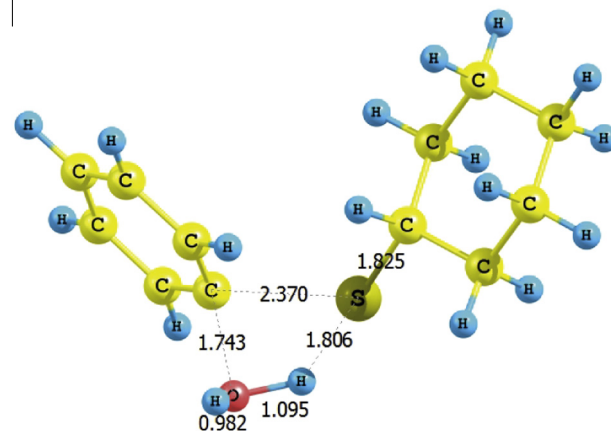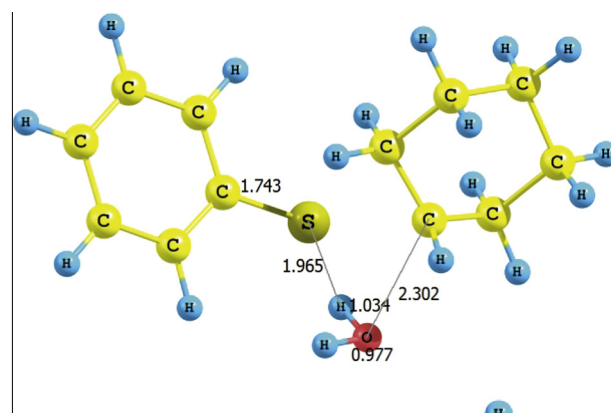
Fig. 4. The geometric structure of transition states for reactions R4 (top) and R5 (bottom), calculated at the PBE/400 level of theory by using VASP program.
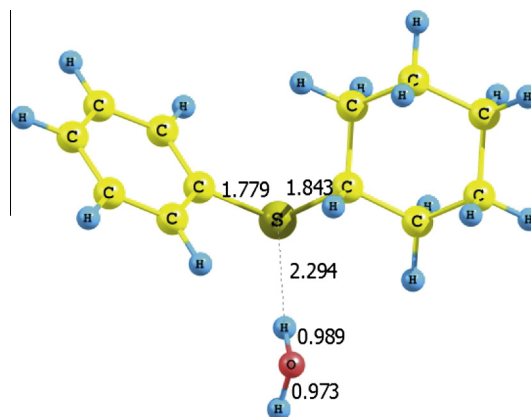
Fig. 5. The geometric structure of complex consisted of reagents for the reactions R4 and R5, calculated at the PBE/400 level of theory by using VASP program.
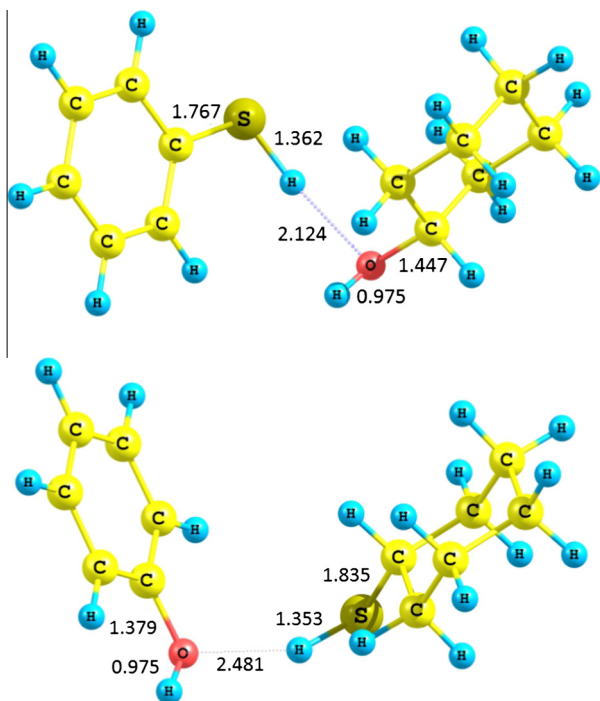
Fig. 6. The geometric structure of complex consisted of products for reactions R4 (top) and R5 (bottom), calculated at the PBE/400 level of theory by using VASP program.

3.5. Solvent effects

The above-mentioned reaction paths were studied for the reactions within the gas phase. In this case the solvent effects are neglected. Meanwhile, the aquathermolysis reaction proceeds in a water environment at high temperature and high pressure [12]. Generally speaking the right way of considering the solvent effects is the application of polarizable continuum model (PCM) to the supermolecule, consisting of reagents, surrounded by a shell of water molecules [34] or use the ONIOM or QM/MM approach for bigger systems (see, for example, Ref. [35]).

In this work in order to estimate the value of solvent effects, we have applied the PCM in the frame of a self-consistent reaction field

Fig. 8. The Gibbs free energy difference (a) and reaction barrier (b) for reactions R4 (red) and R5 (blue), calculated by using GAUSSIAN (.../TZVP) and VASP (.../400) codes in a dependence on the temperature T (K). (For interpretation of the references to color in this figure legend, the reader is referred to the web version of this article.)

(SCRF) [36] by considering the reaction complex without water molecules shell within GAUSSIAN [13] program. We found the transition states for reactions R4 and R5 with optimization of all geometrical parameters at moderate values of dielectric permittivity $\varepsilon = 20$ by using PBE and ωB97XD functionals. It should be emphasized that single imaginary frequencies at transition states of R4 and R5 remained and its value did not change significantly. The change of electron energy contribution to reaction barrier $\Delta E^{\neq}$ after optimization is less than 1 kcal/mol in comparison to unoptimized geometry.

It should be noticed that the value of water dielectric permittivity ε changes from 78 at normal conditions down to a value of about 2 at critical point [37,38]. In order to evaluate the effects of solvent on the Gibbs free energy change ΔG and reaction barrier $\Delta G^{\neq}$, we recalculated the electronic energy E_0 in the range ε from 2 to 80 with a framework of PCM for two reactions – R4 and R5. The corresponding dependencies of ΔE and $\Delta E^{\neq}$ on the dielectric permittivity are given in Fig. 9.

As one can see, the change of electronic energy ΔE does not depend significantly on the dielectric permittivity in both
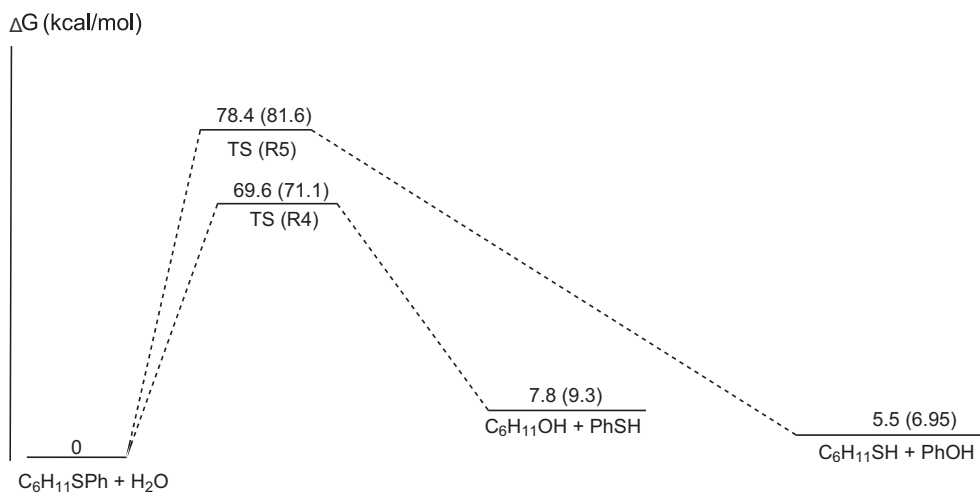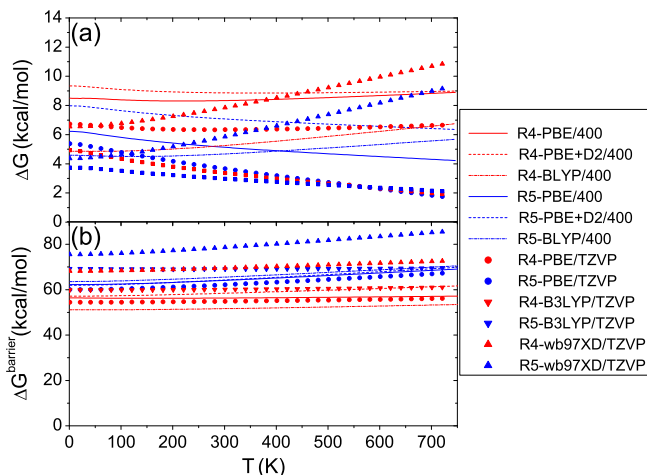

Fig. 7. The energy diagrams for the hydrolysis of cyclohexyl phenyl sulfide (reactions R4 and R5) calculated with respect to the cluster of cyclohexyl phenyl sulfide with one water molecule at the ωB97XD/TZVP level by using the GAUSSIAN program. The values are given for normal conditions (298 K, 1 bar) and also for high pressure–high temperature conditions (523 K, 100 bar, values in parentheses).
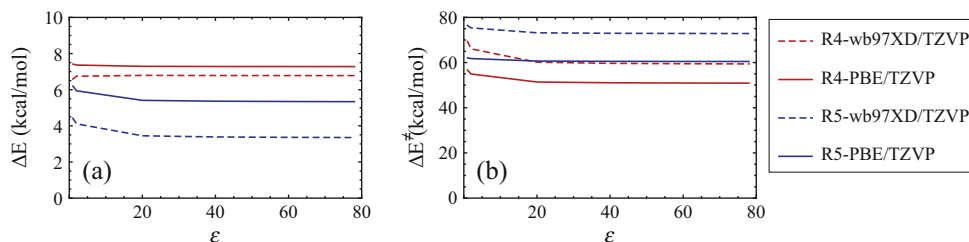
Fig. 9. Change of electronic energy ΔE (a) and electronic energy contribution to reaction barrier $\Delta E^{\neq}$ (b) for reactions R4 and R5 with respect to the solvent dielectric permittivity of ε calculated with GAUSSIAN.

reactions, the magnitude of effect is about 1 kcal/mol in the range of ε from 2 to 80. On the other hand, sensitivity of $\Delta E^{\neq}$ to solvent dielectric permittivity is higher. The maximum change is for barrier of the reaction R4 calculated by ωB87XD/TZVP method – from $\Delta E^{\neq}(\varepsilon = 1) = 69$ kcal/mol to $\Delta E^{\neq}(\varepsilon = 80) = 59$ kcal/mol. The general trends for both reaction barriers is its increasing with decreasing the dielectric permittivity, and as consequence with increasing the temperature. One can notice that because water dielectric constant decreases significantly at specific temperatures of aquathermolysis, the calculations without taking solvent effects into account could be used at least for qualitative comparison of different reaction paths.

3.6. Discussion

The initial steps which determine the kinetics of five different directions of the reactions of cyclohexyl phenyl sulfide in water medium were studied by means of density functional calculations at different levels of theory by using GAUSSIAN and VASP computer codes.

The comparison of electronic energy values (reaction ΔE_0 and activation barriers $\Delta E_0^{\neq}$) is given in Table 2. As one can see, the results of electronic energy values for PBE functional in GAUSSIAN and VASP codes are well comparable. The difference could be explained by using different basis sets. Furthermore, the tendency of electron energy changes for different reactions is the same for all functionals and codes. Moreover, the vibrational contributions (zero point energy, thermal energy and entropy terms, see Eq. (1)) to Gibbs free energy calculated in PBE/400 and PBE/TZVP are coincide as well, as could be seen from Figs. 1, 3 and 8.

Thus, it should be noted that the plane wave approximation gives reliable energetic results which coincide with ones obtained within traditional GAUSSIAN basis sets.

The results of calculations of reaction paths for homolytic cleavage, proton catalyzed cleavage and hydrolysis are summarized in Figs. 10 and 11. The first three reactions were considered by Katritzky and co-authors [12], whereas hydrolysis of cyclohexyl

phenyl sulfide were considered for the first time in the present work.

In the work of Siskin and co-authors [10] it was shown that at 250 °C after 5.5 days 1-methylcyclopentene and thiophenol was formed as major products from cyclohexyl phenyl sulfide. It was also reported that reaction was very accelerated in the presence of an acidic clay (calcium montmorillonite) but that in the presence of a weak base (calcium carbonate) the reactivity was considerably reduced. At 460 °C cyclohexyl phenyl sulfide show extensive reactions after only 7 min [11]. The products vary, but in water medium the major products consists of 1-methylcyclopentene, thiophenol, cyclohexylbenzene and biphenyl. In this medium, desulfurization occurs readily, presumably via acid-catalyzed mechanism, i.e. via the reaction of proton transfer [11] (reaction R3 in the present paper). The similarity of the products between the nonaqueous and aqueous reactions and the varieties of minor products suggest that radical reactions can occur in all cases (reactions R1 and R2 in present paper).

The calculated value of activation energies for homolytic cleavage reaction R1 (45–50 kcal/mol) is directly coincide with the activation energy of Athabasca bitumen thermal cracking reaction (50 kcal/mol) (see [4] and references therein). The slight difference between experimental data and our results could be due to the several reasons: (a) present calculations do not consider the solvent effects for homolytic cleavage; (b) we are considering cyclohexyl phenyl sulfide only as a model compound; (c) generally speaking, thermal cracking includes the cleavage not only of the C–S, but also C–N and C–O hetero bonds.

The results of calculations demonstrate that reaction R3 has the lowest cleavage barrier among the reactions R1–R5 studied in present paper (24 kcal/mol, Figs. 10 and 11). Note that the products of reaction R3 were not observed experimentally in the work of Katritzky et al. [12], there it was shown that the final product of reaction chain started with R3 reaction is 1-methylcyclopenten. It has the largest final yield percentage (in terms of moles and percentage of starting material) equal to 27%. This data is agreed well with the results of our calculations.

Concerning the other routes of reactions of cyclohexyl phenyl sulfide in water medium according to Katritzky et al. [12], the thermal cleavage yields to the formation mostly the thiophenol (11% final yield percentage) rather than cyclohexanethiol (0.3% final yield percentage). This result correlates well with calculated cleavage barriers for reactions R1 (50 kcal/mol) and R2 (70 kcal/mol) respectively.

As could be seen from Table 2 and Fig. 11, addition of the water molecule as a reagent in reaction R4 and R5 leads to the lowering of reaction barrier in comparison to R1 and R2 reactions at low temperatures. These results are in agreement with the results of Ref. [7], where it was established that decomposition barrier of HCOOH (64.6 kcal/mol) is lowered by 30% in the presence of one water molecule (45.5 kcal/mol), by 50% in the presence of two water molecules (34.7 kcal/mol) and by 60% in the presence of another HCOOH molecule (26.7 kcal/mol). Thus, the water molecules could act as a catalyst.

Table 2
Comparison of the electronic energy values (reaction energy change ΔE_0 and activation barriers $\Delta E_0^{\neq}$ with respect to pre-reaction complexes, in kcal/mol) for the reactions of thermal cleavage (R1, R2), proton catalyzed cleavage (R3) and hydrolysis (R4, R5).

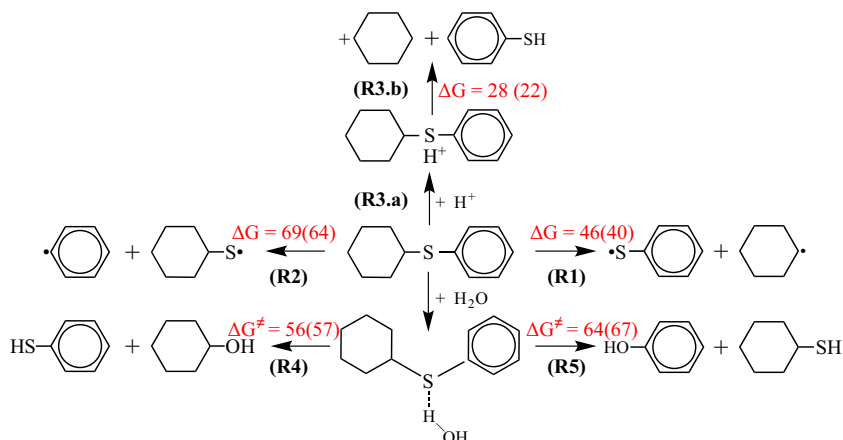| Reaction	Energy	GAUSSIAN			VASP		
		PBE	B3LYP	ωb97XD	PBE	PBE + D2	BLYP
R1	ΔE_0	61.5	64.9	74.8	61.8	66.8	52.4
R2	ΔE_0	83.4	77.6	86.0	84.2	88.4	75.8
R3.b	ΔE_0	43.6	38.6	47.9	38.2	43.2	27.6
R4	ΔE_0	7.4	6.3	6.6	9.0	9.8	5.3
	$\Delta E_0^{\neq}$	56.6	61.9	69.3	58.4	58.9	52.9
R5	ΔE_0	6.2	4.8	4.4	6.7	8.6	5.0
	$\Delta E_0^{\neq}$	62.0	70.6	76.4	64.5	64.2	65.7

Fig. 10. The results of calculations of reaction paths for the homolytic cleavage (R1 and R2), proton catalyzed cleavage (R3.a and R3.b) and hydrolysis (R4 and R5) of cyclohexyl phenyl sulfide in aqueous media at the PBE/400 level of theory. The free energy change ΔG and reaction barrier height $\Delta G^{\neq}$ are given in kcal/mol at temperature $T = 298$ K (525 K in parentheses).
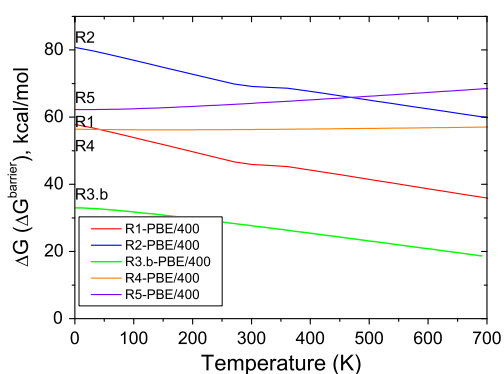

Fig. 11. The Gibbs free energy change/reaction barrier for reactions R1–R5, calculated at the PBE/400 level of theory in a dependence on the temperature T (K).

We have analyzed the temperature influence on the reactions barriers. As could be seen from Fig. 11, proton catalyzed reaction mechanism (R3) is a major route in process of cyclohexyl phenyl sulfide aquathermolysis at the condition of sufficient hydrogen ion H$^+$ concentration in whole temperature range. With increasing the temperature above the critical point, H$^+$ concentration decreases and thermal cracking (R1) should become a dominant process. Also, there is a tendency that at low temperatures hydrolysis reaction (R4) is more preferable than thermal cracking (R1). This is confirmed by the experimental data [11], which shows that at 250 °C cyclohexyl phenyl sulfide underwent cleavage faster under aqueous conditions (ionic pathway) than under thermal conditions (radical pathway).

4. Conclusions

In the present paper we have studied on the molecular level a number of mechanisms of aquathermolysis reactions, including C–S heterobond cleavage: thermal cracking (R1, R2), proton catalyzed cracking (R3) and hydrolysis (R4, R5). We have considered water molecules as a reagent (reactions R4 and R5) and its ions (H$_3$O$^+$) as a catalyst (reaction R3).

Firstly, it was established, that thermal cracking (reactions R1 and R2) of these compounds needs a big amount of energy (which is rather probable at the conditions of oil formation) and could happen only at harsh reaction conditions.

Secondly, catalytic reaction with involvement of hydrogen cation is most favorable for the formation and transformation of thiophenyl-sec-alkyl (tert-alkyl) radicals and reduces the energy required to break the C–S heterobond significantly.

Thirdly, the presence of water in the reaction is a key point. The process of its involvement in various reactions with radical particles becomes more favorable. In that case one could obtain another synthetically significant results, such as the formation of phenols and alkanols. Addition of water directs reaction on kinetically-controlled path. If water is not available, then the reactions of isomerization, recombination and other typical processes of radical transformations starts. In terms of production, radicals are formed at high temperatures during the oil treatment as well as at extreme conditions in oil reservoir.

The obtained results could be useful for the systems like tert-alkyl (secondary-alkyl) thiophenyl ethers, which could be formed in heavy oils at extreme conditions.

Concerning the predictive capabilities, our results could be used to assess the feasibility of different reactions directions, as well as rates and energetic parameters of chemical compounds which contain branched alkyl and aryl groups at the sulfur atom.

We have shown that *ab initio* methods could give us the correct trends and tendencies for possible chemical reactions paths on base of model compounds, such as cyclohexyl phenyl sulfide with water molecule, thereby we have demonstrated its applicability for comparative studies of chemical reaction pathways in an aquathermolysis processes. Theoretical analysis of reactions paths based on the results of *ab initio* calculations are an obligatory condition for comprehensive understanding of the chemical reaction mechanisms, especially when catalysts are involved. The efficiency of catalysts is associated with the decreasing of the reaction barriers. We have presented the scheme of different reaction directions with corresponding calculated values of reaction barriers, which map onto experimental trends, and could be used for comparison with other reaction mechanisms.

Appendix A. Supplementary material

Supplementary data associated with this article can be found, in the online version, at http://dx.doi.org/10.1016/j.comptc.2016.01.008.

References

[1] J. Hyne, J. Greidanus, J. Tyrer, D. Verona, C. Rizek, P. Clark, R. Clarke, J. Koo, The Second International Conference on Heavy Crude and Tar Sands, 1982, p. 82.

[2] J. Hyne, P. Clark, R. Clarke, J. Koo, J. Greidanus, J. Tyrer, D. Verona, Aquathermolysis of heavy oils, Rev. Tec. INTEVEP 2 (1982) 87–94.

[3] S. Maity, J. Ancheyta, G. Marroquín, Catalytic aquathermolysis used for viscosity reduction of heavy crude oils: a review, Energy Fuels 24 (2010) 2809–2816.

[4] P.R. Kapadia, M.S. Kallos, I.D. Gates, A review of pyrolysis, aquathermolysis, and oxidation of Athabasca bitumen, Fuel Process. Technol. 131 (2015) 270–289.

[5] P.E. Savage, Organic chemical reactions in supercritical water, Chem. Rev. 99 (1999) 603–621.

[6] M. Siskin, A.R. Katritzky, Reactivity of organic compounds in superheated water: general background, Chem. Rev. 101 (2001) 825–836.

[7] B. Wang, H. Hou, Y. Gu, New mechanism for the catalyzed thermal decomposition of formic acid, J. Phys. Chem. A 104 (2000) 10526–10528.

[8] J.R. Gomes, M.A. Ribeiro da Silva, Thermochemistry of small organosulfur compounds from ab initio calculations, J. Phys. Chem. A 108 (2004) 11684–11690.

[9] V. Lyubimenko, N. Petrukhina, B. Tumanyan, I. Kolesnikov, Thermodynamic parameters of conversion reactions of some heavy oil components under the action of steam and heat, Chem. Technol. Fuels Oils 48 (2012) 292–301.

[10] M. Siskin, G. Brons, A.R. Katritzky, R. Murugan, Aqueous organic chemistry. 2. Crosslinked cyclohexyl phenyl compounds, Energy Fuels 4 (1990) 482–488.

[11] A.R. Katritzky, R.A. Barcock, M. Balasubramanian, J.V. Greenhill, M. Siskin, W.N. Olmstead, Aqueous high-temperature chemistry of carbo-and heterocycles. 21. Reactions of sulfur-containing compounds in supercritical water at 460 °C, Energy Fuels 8 (1994) 498–506.

[12] A.R. Katritzky, D.A. Nichols, M. Siskin, R. Murugan, M. Balasubramanian, Reactions in high-temperature aqueous media, Chem. Rev. 101 (2001) 837–892.

[13] M.J. Frisch, G.W. Trucks, H.B. Schlegel, G.E. Scuseria, M.A. Robb, J.R. Cheeseman, J.A. Montgomery Jr., T. Vreven, K.N. Kudin, J.C. Burant, J.M. Millam, S.S. Iyengar, J. Tomasi, V. Barone, B. Mennucci, M. Cossi, G. Scalmani, N. Rega, G.A. Petersson, H. Nakatsuji, M. Hada, M. Ehara, K. Toyota, R. Fukuda, J. Hasegawa, M. Ishida, T. Nakajima, Y. Honda, O. Kitao, H. Nakai, M. Klene, X. Li, J.E. Knox, H. P. Hratchian, J.B. Cross, V. Bakken, C. Adamo, J. Jaramillo, R. Gomperts, R.E. Stratmann, O. Yazyev, A.J. Austin, R. Cammi, C. Pomelli, J.W. Ochterski, P.Y. Ayala, K. Morokuma, G.A. Voth, P. Salvador, J.J. Dannenberg, V.G. Zakrzewski, S. Dapprich, A.D. Daniels, M.C. Strain, O. Farkas, D.K. Malick, A.D. Rabuck, K. Raghavachari, J.B. Foresman, J.V. Ortiz, Q. Cui, A.G. Baboul, S. Clifford, J. Cioslowski, B.B. Stefanov, G. Liu, A. Liashenko, P. Piskorz, I. Komaromi, R.L. Martin, D.J. Fox, T. Keith, M.A. Al-Laham, C.Y. Peng, A. Nanayakkara, M. Challacombe, P.M.W. Gill, B. Johnson, W. Chen, M.W. Wong, C. Gonzalez, J.A. Pople, Gaussian 03, Gaussian, Inc., Wallingford, CT, 2004.

[14] G. Kresse, J. Hafner, Ab initio molecular dynamics for liquid metals, Phys. Rev. B 47 (1993) 558.

[15] G. Kresse, J. Hafner, *Ab initio* molecular-dynamics simulation of the liquid-metal amorphous-semiconductor transition in germanium, Phys. Rev. B 49 (1994) 14251–14269.

[16] G. Kresse, J. Furthmuller, Efficiency of ab-initio total energy calculations for metals and semiconductors using a plane-wave basis set, Comput. Mater. Sci. 6 (1996) 15–50.

[17] G. Kresse, J. Furthmuller, Efficient iterative schemes for *ab initio* total-energy calculations using a plane-wave basis set, Phys. Rev. B 54 (1996) 11169–11186.

[18] J.P. Perdew, K. Burke, M. Ernzerhof, Generalized gradient approximation made simple, Phys. Rev. Lett. 77 (1996) 3865–3868.

[19] C. Lee, W. Yang, R.G. Parr, Development of the Colle–Salvetti correlation-energy formula into a functional of the electron density, Phys. Rev. B 37 (1988) 785–789.

[20] A.D. Becke, Density-functional thermochemistry. III. The role of exact exchange, J. Chem. Phys. 98 (1993) 5648–5652.

[21] T.H. Dunning Jr., Gaussian basis functions for use in molecular calculations. III. Contraction of (10s6p) atomic basis sets for the first-row atoms, J. Chem. Phys. 55 (1971) 716–723.

[22] A. Schäfer, H. Horn, R. Ahlrichs, Fully optimized contracted gaussian basis sets for atoms Li to Kr, J. Chem. Phys. 97 (1992) 2571–2577.

[23] A. Schäfer, C. Huber, R. Ahlrichs, Fully optimized contracted gaussian basis sets of triple zeta valence quality for atoms Li to Kr, J. Chem. Phys. 100 (1994) 5829–5835.

[24] J.-D. Chai, M. Head-Gordon, Long-range corrected hybrid density functionals with damped atom–atom dispersion corrections, Phys. Chem. Chem. Phys. 10 (2008) 6615–6620.

[25] K. Fukui, The path of chemical reactions-the IRC approach, Acc. Chem. Res. 14 (1981) 363–368.

[26] D.A. McQuarrie, J.D. Simon, Molecular Thermodynamics, vol. 450, University Science Books, Sausalito, CA, 1999.

[27] G. Kresse, D. Joubert, From ultrasoft pseudopotentials to the projector augmented-wave method, Phys. Rev. B 59 (1999) 1758–1775.

[28] S. Grimme, Semiempirical GGA-type density functional constructed with a long-range dispersion correction, J. Comput. Chem. 27 (2006) 1787–1799.

[29] B. Miehlich, A. Savin, H. Stoll, H. Preuss, Results obtained with the correlation energy density functionals of Becke and Lee, Yang and Parr, Chem. Phys. Lett. 157 (1989) 200–206.

[30] K. Parlinski, Z.Q. Li, Y. Kawazoe, First-principles determination of the soft mode in cubic ZrO_2, Phys. Rev. Lett. 78 (1997) 4063–4066.

[31] G. Mills, H. Jónsson, Quantum and thermal effects in h_2 dissociative adsorption: evaluation of free energy barriers in multidimensional quantum systems, Phys. Rev. Lett. 72 (1994) 1124–1127.

[32] Y.-R. Luo, Comprehensive Handbook of Chemical Bond Energies, CRC Press, Boca Raton, FL, 2007.

[33] A.R. Katritzky, S.M. Allin, M. Siskin, Aquathermolysis: reactions of organic compounds with superheated water, Acc. Chem. Res. 29 (1996) 399–406.

[34] R. Aminova, E. Baisupova, A. Aganov, Calculations of 31p magnetic shielding constants of derivatives of betaine and phosphine molecules dissolved in different solvents by using supermolecular model and combined methods of quantum chemistry and molecular mechanics, Appl. Magn. Reson. 40 (2011).

[35] X. Liu, D.R. Salahub, Molybdenum carbide nanocatalysts at work in the in situ environment: a density functional tight-binding and quantum mechanical/molecular mechanical study, J. Am. Chem. Soc. 137 (2015) 4249–4259.

[36] J. Tomasi, B. Mennucci, R. Cammi, Quantum mechanical continuum solvation models, Chem. Rev. 105 (2005) 2999–3094.

[37] M. Uematsu, E. Frank, Static dielectric constant of water and steam, J. Phys. Chem. Ref. Data 9 (1980) 1291–1306.

[38] V. Kulinskii, N. Malomuzh, Properties of water near its critical point, in: Soft Matter Under Exogenic Impacts, Springer, 2007, pp. 287–304.